LEGIBILITY NOTICE

A major purpose of the Technical Information Center is to provide the broadest dissemination possible of information contained in DOE's Research and Development Reports to business, industry, the academic community, and federal, state and local governments.

Although a small portion of this report is not reproducible, it is being made available to expedite the availability of information on the research discussed herein.

LA-UR -87-2147

CONF-8709110--1

LA-UR--87-2147

DE87 011740

TITLE SIDEBAND SUPPRESSION BY AN INTRACAVITY OPTICAL FILTER IN THE LOS ALAMOS FREE-ELECTRON LASER OSCILLATOR

AUTHOR(S) John C. Goldstein, Brian E. Newnam, and Roger W. Warren

SUBMITTED TO Ninth International Free-Electron Laser Conference to be held in Williamsburg, VA, September 14-18, 1987.

MASTER

Los Alamos Los Alamos National Laboratory Los Alamos, New Mexico 87545

FORM NO 836 R4
ST NO 2629 5/81

DISTRIBUTION OF THIS DOCUMENT IS UNLIMITED

Sideband Suppression by an Intracavity Optical Filter in the Los Alamos Free-Electron Laser Oscillator*

John C. Goldstein, Brian E. Newnam, and Roger W. Warren
Group X-1, MS E531
Los Alamos National Laboratory
Los Alamos, NM 87545
505/667-4370

ABSTRACT

Experiments at the Los Alamos free-electron laser oscillator were performed with a 7.35% ($\Delta\gamma_r/\gamma_r$) tapered wiggler. Multilayer dielectric mirrors with wavelength-dependent reflectivity and phase shift functions were used to provide high reflectivity at the fundamental wavelength but to introduce losses at expected sideband wavelengths. The electron-beam energy was varied to tune the fundamental optical wavelength. Experimental measurements are compared with results of 1-d time-dependent simulations. For the particular wiggler, optics, and e-beam conditions of this experiment, spectral sidebands were reduced only with a concomitant reduction of the total optical output of the laser.

I. INTRODUCTION

At the time of the development of one of the first theoretical treatments of tapered-wiggler free-electron lasers (FELs), it was recognized[1] that the nonlinear response of electrons to a strong monochromatic optical driving field could result in the generation of light at wavelengths displaced from that of the driving field. The new components in the optical spectrum were called Raman sidebands because the process of generation of these components was somewhat analogous to an atomic or molecular Raman scattering process. It was also recognized[1] that this process could prevent achievement of high extraction efficiencies in tapered-wiggler FELs and that some type of frequency discrimination - i.e., wavelength-dependent resonator losses which are higher at sideband wavelengths than at the design wavelength - would be a practical way of reducing or eliminating the unwanted parasitic wavelengths.

The 1-d pulse propagation model for FEL oscillators[2] contained a self-consistent treatment of the interaction of the optical field and the electrons. Solution of this mathematical model for tapered-wiggler oscillators[3,4] showed the development of sidebands. However, solution of the model for untapered-wiggler oscillators[5,6] also showed substantial

*Work performed under the auspices of the U.S. Department of Energy and supported by the U.S. Army Ballistic Missile Defense Organization.

sideband generation which increased the total power output of the laser over that predicted without allowing for multimode optical fields.[1] Recent pulse evolution calculations for oscillators with strongly-tapered-wigglers,[7,8,9] which operate at intensities that correspond to several synchrotron periods over the length of the wiggler, show clearly that sidebands are deleterious and must be eliminated in order to achieve the design extraction efficiency. The present theoretical view is that sideband generation leads to greater power output in untapered, or weakly-tapered, wiggler oscillators, but must be eliminated in strongly-tapered-wiggler devices that operate at very high intensity if the full design performance of those wigglers is to be realized.

The present work presents a study of the effect of eliminating or reducing sidebands in a modestly tapered-wiggler oscillator. Sidebands were reduced by using the wavelength-dependent reflectivity of multilayer dielectric mirrors to introduce losses at expected sideband wavelengths. The wavelength of the FEL oscillator was adjusted by varying the mean energy of the electron beam. Data was collected for a series of wavelengths which approached the reflectivity edge of the mirrors. These data will be compared with the results of 1-d time-dependent numerical simulations. Previous experiments[10], which used an untapered wiggler and dielectric mirrors with slightly different characteristics, resulted in a reduction of the total laser output as the sidebands were quenched. Although these results were not compared to theoretical simulations, they are in qualitative agreement with previous theoretical calculations.[5,6]

II. EXPERIMENTS

The layout, operating conditions, and diagnostics of the Los Alamos free-electron laser oscillator have been previously described in detail.[11,12] The tapered wiggler was the same as had been used in the FEL amplifier experiment[13] and also has been previously described in detail[13,14]: it is a 1-m long plane-polarized wiggler made from $SmCo_5$ magnets with an approximately linearly tapered wavelength (2.73 cm to 2.42 cm) and a constant field (~0.3 T) as shown in Fig. 1. The 11% taper in wavelength corresponds to a fractional change in the energy of the resonant particle ($\Delta\gamma_r/\gamma_r$) of 7.35%.

For this experiment, two dielectric mirrors made from seven quarter-wave thick pairs of $ZnSe/ThF_4$ coatings deposited on a ZnSe substrate were used. The mirrors had radii of curvature of 3.80m and 3.39m and were separated by about 6.92m. Aside from different radii of curvature, the mirrors were identical and each had a measured reflectivity maximum of 99.4% at an optical wavelength of 10.6μm. At longer wavelengths, the reflectivity dropped, and the transmission increased until it reached 10% at λ_c=12.6μm. Further details of the wavelength dependence of these mirrors are discussed below in section III.

The electron beam conditions were similar to those previously reported[11,12]: 40-A peak current in a 30-ps (FWHM) pulse with a fractional energy spread of about 1% and an rms absolute emittance of about $3\pi \times 10^{-4}$ cm•rad.

The experiment measured the total energy in light emitted by the laser over the duration of the electron-beam macropulse. The operating wavelength λ of the FEL was varied by changing the mean energy of the electrons from the linac. Figure 2 shows these data plotted versus the wavelength difference $\Delta\lambda=\lambda_c-\lambda$.

These measurements were accompanied by time-integrated (over the macropulse) optical spectrum measurements. The spectral measurements showed great shot-to-shot variability: the displacement of the spectrum to longer wavelengths as the electron-beam energy was reduced was apparent, as was a reduction of the width and complexity of the spectra as the laser threshold was approached. This is in agreement with similar data for the untapered wiggler[10] which clearly showed a spectral narrowing as the reflectivity edge of the mirror was approached. The results of simulations of this experiment also show the expected spectral narrowing and are discussed below.

III. THEORETICAL CALCULATIONS

One-dimensional, time-dependent, pulse-evolution calculations were performed for the conditions of this experiment. The calculations used the mathematical model of Ref. 14 supplemented with wavelength-dependent mirrors: the reflectivity, phase shift, and transmission (there were small but finite absorption losses) versus optical wavelength used in the code are shown in Fig. 3. Note that both mirrors were assumed to have identical characteristics, and Figs. (3a) and (3b) refer to the effects of two consecutive reflections upon the electric field amplitude of the optical pulse.

The effects of the mirrors upon the optical pulse were taken into account in the numerical calculations by the following procedure: the spatial Fourier transform of the pulse at the end of the wiggler was calculated, then multiplied by the wavelength dependent amplitude and phase shift shown in Fig. 3, and then the resultant function was inverse-Fourier-transformed to obtain the pulse for the next pass through the wiggler.

The transmission of each mirror as a function of wavelength was measured separately with a Beckman IR spectrometer. A commercially available computer code[15] was used, together with the known composition of the mirrors, to compute the spectral characteristics (reflectance, transmittance, and phase shift) of the mirrors. The measured transmission data could not be exactly matched by any calculation of this code, possibly because of small deviations from quarter-wave layer thicknesses. Therefore, the phase shift from the calculation which most closely fit the transmission data was used in the FEL simulations, but calculated values of the reflectivity and transmission were changed slightly to bring them into better agreement with the measurements. The calculated laser performance is very sensitive to the shape of the reflectivity vs. wavelength curve, and this curve is only approximately represented in the simulation model.

The oscillator performance was calculated for three different wavelengths of peak small-signal gain: $\lambda_1=11.8$ μm ($\gamma_0=38.49$), $\lambda_2=12.1\mu$m ($\gamma_0=38.01$), and $\lambda_3=12.35\mu$m ($\gamma_0=37.626$). The calculations were all done for a parabolic electron pulse shape, FWHM equal to 30 ps, and peak current 40A. A 2% wide electron energy spread (rectangular, not Gaussian, in shape) was used - this includes approximately equal contributions from the $3\pi \times 10^{-4}$ cm•rad rms transverse emittance and 1% real energy spread. These parameter values yield a maximum small-signal gain of about 10%.

The calculated optical output energies versus wavelength of peak small-signal gain are shown in Fig. 4 along with the measured data. Although the trends are similar, there is substantial quantitative disagreement between the calculated and measured curves. Possible reasons for the discrepancy are discussed below in the next section.

Some additional features of the calculated results are shown in the next several figures. Figure 5 shows the time-integrated optical spectra for the three cases. One notes a narrowing of the spectra as the initial wavelength approaches the laser threshold: no sidebands developed for $\lambda=\lambda_3$. The calculations all started with spontaneous emission (a different mathematical model than that of Ref. 14) and zero initial optical intensity. The growth of the optical pulse energy inside the optical cavity versus pass number is shown for the three cases in Fig. 6: the duration (100μs) of the electron beam macropulse from the linac corresponded to 2000 round trips of the optical pulse in the resonator. Note that for $\lambda=\lambda_3$ a steady-state was not achieved in the available time.

IV. DISCUSSION AND CONCLUSIONS

There are two general considerations that arise whenever 1-d time-dependent simulations have been compared with experimentally-measured results from the Los Alamos free-electron laser oscillator experiment[10,16]: (a) the simulations do not include three-dimensional effects, and (b) it is difficult to determine experimentally the values of many different parameters needed to do the simulations. A further point is that some electron-beam parameters vary during the macropulse, either as slow drifts or as random fluctuations: although calculations have been done to model such effects upon FEL performance, they were not included in the present simulations. Furthermore, some measured properties are usually simplified in the simulations in order to make the computer calculations tractable.

The primary three-dimensional effect not included in the calculations is the spatial overlap between the transverse dimensions of the electron beam - which are determined by the value of the transverse emittance and the properties of the wiggler - and the transverse dimensions of the light beam - which are determined by the optical wavelength and the Rayleigh range of the resonator. Using a value of $3\pi \times 10^{-4}$ cm•rad for the rms transverse emittance (not very precisely measured), 12μm optical wavelength, and a Rayleigh range of 50 cm, the focal diameters of the two beams are about the same. This means that the basic assumption of the 1-d model - that all electrons are acted upon by the on-axis component of the optical field - is certainly not satisfied. One expects that better calculations[17] would substantially reduce the optical output due to this effect. Unfortunately, the approach of Ref. 17 cannot be used to model the evolution of a finite pulse in an FEL oscillator due to practical computer time limitations.

Parameter values for the wiggler and the optical resonator are normally accurately determined and constant during the experiment - but note the difficulty in this experiment of precisely determining the exact wavelength-dependent properties of the mirrors, as described in Sec. III.

Parameters for the electron-beam are usually most elusive: effects not quantitatively specified here experimentally, and not included in the simulations, include a ramp on the current during the macropulse, a slow drift of the mean electron energy during the macropulse, and electron micropulse arrival-time fluctuations due to accelerator field fluctuations. Such effects have been studied previously[12,16,18] and tend to reduce the laser output. Slow drifts can easily be included in the simulations if they are known for a particular output measurement; fluctuations can be included but no adequate model for their statistics has been developed. If the peak micropulse current decreased during the macropulse, as happened on some shots, obviously that would lead to diminished output. Slow energy drifts and rapid fluctuations might further reduce the output. Finally, shot-to-shot variations of the mean e-beam energy, thought to be on the order of $\pm 1/4\%$ to $\pm 1/3\%$, would mean that the theoretical curve of Fig. 2 should be averaged over $\pm 1/2\%$ to $\pm 2/3\%$ wavelength ranges.

The general experimental and theoretical conclusions of the present study of this tapered-wiggler FEL oscillator are that: (1) sidebands were generated when the fundamental optical wavelength was in the high-reflectivity part of the mirror response; and (2) the total optical laser energy output dropped, and the time-integrated optical output spectrum narrowed, as the fundamental wavelength was tuned to values corresponding to decreased mirror reflectivity.

There are, however, substantial quantitative differences between the calculations and the measurements. We believe that the largest contribution to these differences comes from not having done 3-d simulations that properly treat the transverse overlap of the optical and electron beams. Electron beam variations, which were not included in the calculations either, would further reduce calculated laser output values. A better knowledge of the mirror characteristics to use in the calculations would probably lead to relatively minor changes in the calculated results.

REFERENCES

1. N.M. Kroll, P.L. Morton, and M.N. Rosenbluth, "Free-Electron Lasers With Variable Parameter Wigglers," IEEE J. Quant. Electron. QE-17, pp.1436-1468 (1981).

2. W.B. Colson and S.K. Ride, "The Free-Electron Laser: Maxwell's Equations Driven by Single-particle Currents," in Free-Electron Generators of Coherent Radiation, Physics of Quantum Electronics Vol. 7, S.F. Jacobs, H.S. Pilloff, M. Sargent III, M.O. Scully, and R. Spitzer, Eds. (Addison-Wesley, 1980), p.377.

3. W.B. Colson, "Optical Pulse Evolution in the Stanford Free-Electron Laser and in a Tapered Wiggler," in Free-Electron Generators of Coherent Radiation, Physics of Quantum Electronics Vol. 8, S.F. Jacobs, G.T. Moore, H.S. Pilloff, M.Sargent III, M.O. Scully, and R. Spitzer, Eds. (Addison-Wesley, 1982), pp. 457-488.

4. J.C. Goldstein and W.B. Colson, "Pulse Propagation in Free-Electron Lasers with a Tapered Undulator," in Proceedings of the International Conference on Lasers '81, C.B. Collins ed., (STS Press, 1982), p.93.

5. W.B. Colson and A. Renieri, "Pulse Propagation in Free-Electron Lasers," J. de Physique, Colloque C1, pp.11-28 (February, 1983).

6. R.W. Warren, J.C. Goldstein, and B.E. Newnam, "Spiking Mode Operation for a Uniform-Period Wiggler," Nucl. Instr. and Meth. in Phys. Res. A250, pp. 19-25 (1986).

7. D.C. Quimby, J.M. Slater, and J.P. Wilcoxon, "Sideband Suppression in Free-Electron Lasers With Multiple Synchrotron Periods," IEEE J. Quant. Electron. QE-21, p.979 (1985).

8. H. Takeda, B.D. McVey, and J.C. Goldstein, "Theoretical Study of a High Extraction Efficiency Undulator for a Free-Electron Laser Oscillator," 8th Int. FEL Conference, Glasgow, Scotland, 9/1-5/86, to be published in Nucl. Instr. and Meth. for Phys. Research.

9. R.L. Tokar, B.D. McVey, and J.C. Goldstein, "Sideband Suppression in Free-Electron Lasers using a Grating Rhomb," to be published.

10. R.W. Warren, B.E. Newnam, and J.C. Goldstein, "Raman Spectra and the Los Alamos Free-Electron Laser," IEEE J. Quant. Electron. QE-21, pp. 882-888 (1985).

11. B.E. Newnam, R.W. Warren, R.L. Sheffield, J.C. Goldstein, and C.A. Brau, "The Los Alamos Free-Electron Laser: Optical Performance," Nucl. Instr. and Meth. in Phys. Res. A237, pp. 187-198 (1985).

12. B.E. Newnam, R.W. Warren, R.L. Scheffield, W.E. Stein, M.T. Lynch, J.S. Fraser, J.C. Goldstein, J.E. Sollid, T.A. Swann, J.M. Watson, and C.A. Brau, "Optical Performance of the Los Alamos Free-Electron Laser," IEEE J. Quant. Electron. QE-21, pp. 867-881 (1985).

13. R.W. Warren, B.E. Newnam, J.G. Winston, W.E. Stein, L.M. Young, and C.A. Brau, "Results of the Los Alamos Free-Electron Laser Experiment," IEEE J. Quant. Electron QE-19, pp. 391-400 (1983).

14. J.C. Goldstein, "Evolution of Long Pulses in a Tapered Wiggler Free-Electron Laser," in Free Electron Generators of Coherent Radiation, Proc. SPIE 453, C.A. Brau, S.F. Jacobs, and M.O. Scully eds., pp. 2-10 (1984).

15. "Macleod," a thin-film code written by Angus Macleod of the University of Arizona, Tucson, Arizona.

16. J.C. Goldstein, B.E. Newnam, R.W. Warren, and R.L. Sheffield, "Comparison of the Results of Theoretical Calculations with Experimental Measurements from the Los Alamos Free-Electron Laser Oscillator Experiment," Nucl. Instr. and Meth. in Phys. Res. A250, pp. 4-11 (1986).

17. B.D. McVey, "Three-Dimensional Simulations of Free-Electron Laser Physics," Nucl. Instr. and Meth. in Phys. Res. A250, pp. 449-455 (1986).

18. M.T. Lynch, R.W. Warren, and P.J. Tallerico, "The Effects of Linear-Accelerator Noise on the Los Alamos Free-Electron Laser," IEEE J. Quant. Electron. QE-21, pp. 904-908 (1985).

Figure Captions

Fig. 1. Tapered wiggler magnetic field amplitude and wavelength vs. axial position.

Fig. 2. Measured laser optical output energy vs. wavelength.

Fig. 3a. Electric field amplitude reflection coefficient vs. wavelength.

Fig. 3b. Electric field phase shift coefficient vs. wavelength.

Fig. 3c. Single mirror intensity transmission coefficient vs. wavelength.

Fig. 4. Calculated and measured optical output energy vs. wavelength.

Fig. 5a. Time-integrated output optical spectrum at λ_1=11.8 μm.

Fig. 5b. Time integrated output optical spectrum at λ_2=12.1 μm.

Fig. 5c. Time-integrated output optical spectrum at λ_3=12.35 μm.

Fig. 6a. Internal optical pulse energy vs. pass number for $\lambda = \lambda_1$.

Fig. 6b. Internal optical pulse energy vs. pass number for $\lambda = \lambda_2$.

Fig. 6c. Internal optical pulse energy vs. pass number for $\lambda = \lambda_3$.

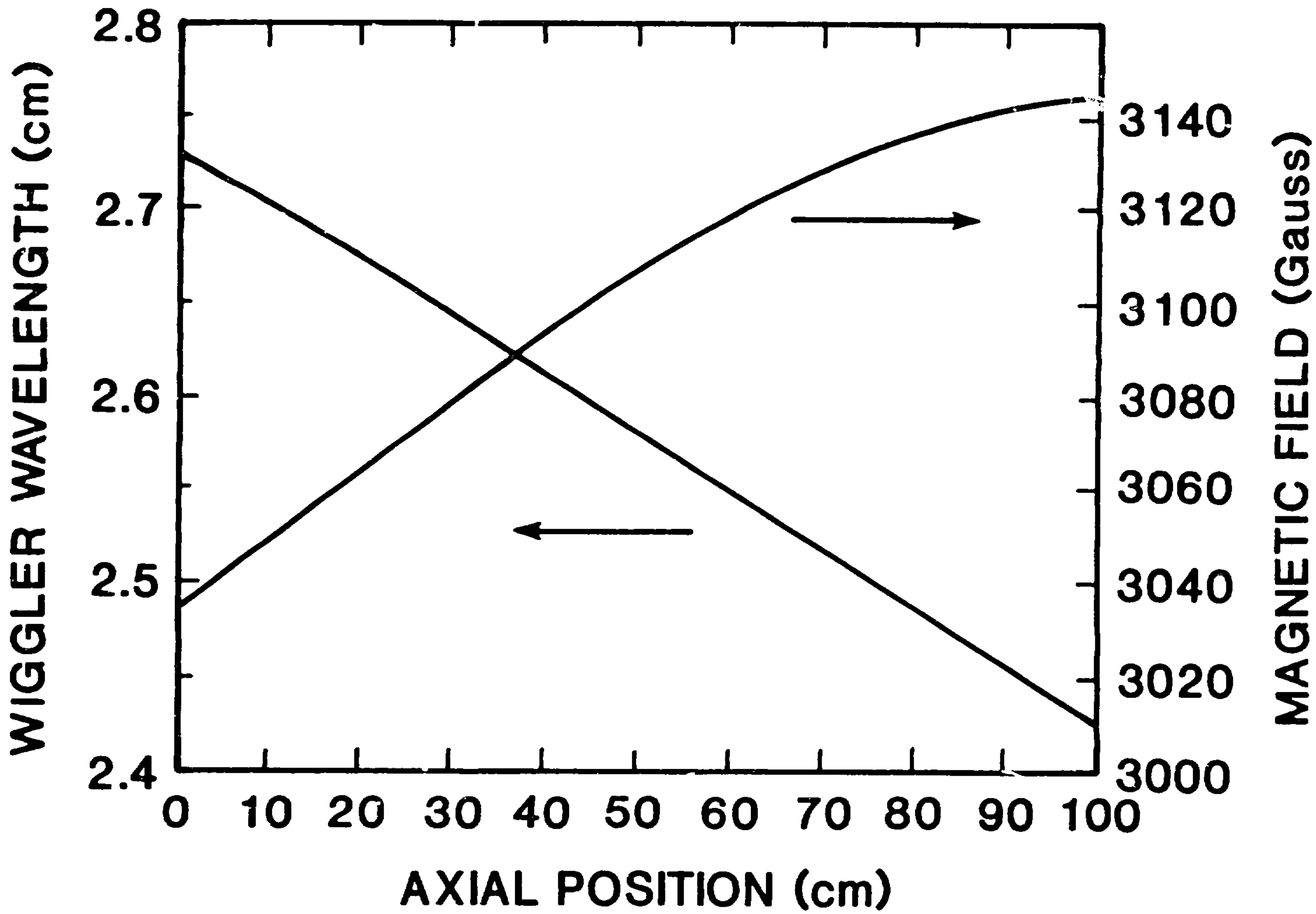
2.8
2.7
2.6
2.5
2.4
WIGGLER WAVELENGTH (cm)
3140
3120
3100
3080
3060
3040
3020
3000
MAGNETIC FIELD (Gauss)
0
10
20
30
40
50
60
70
80
90
100
AXIAL POSITION (cm)

Figure 1

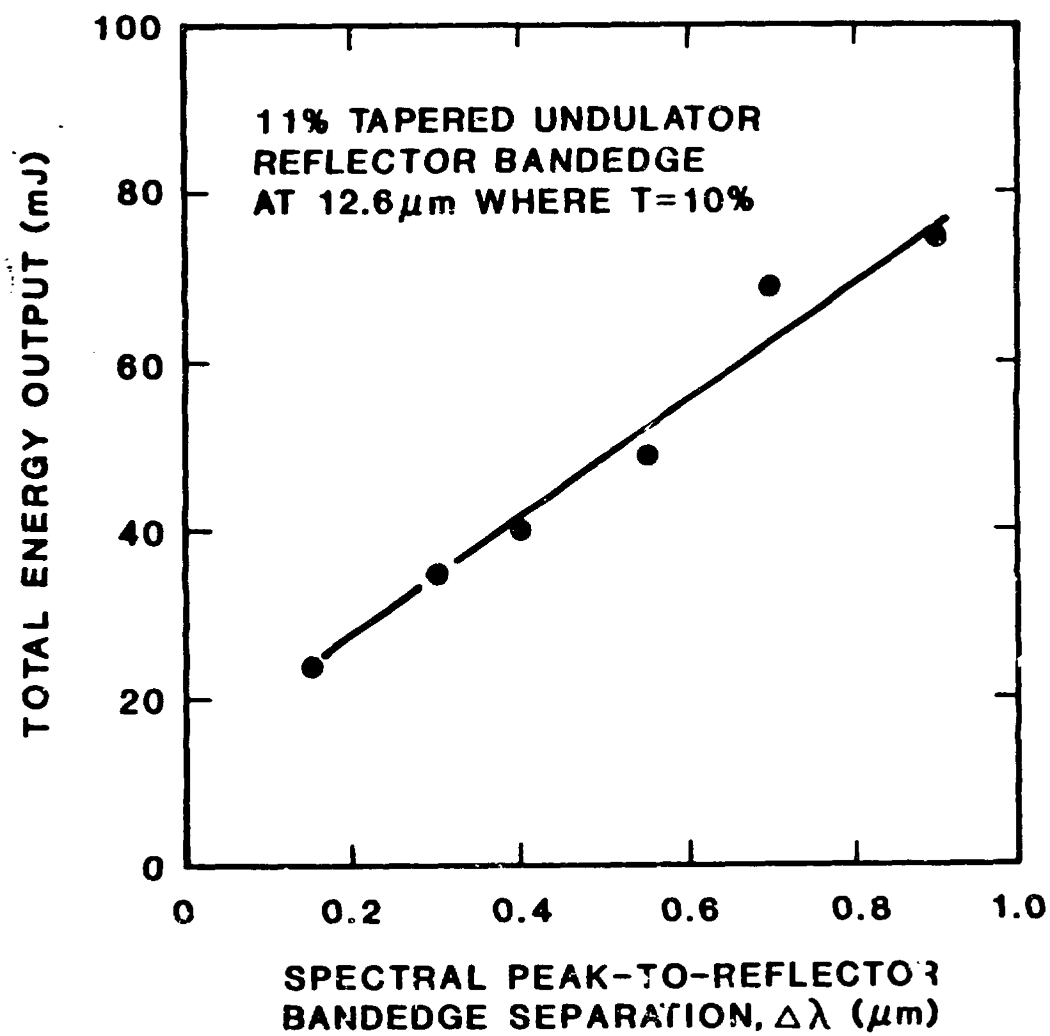

11% TAPERED UNDULATOR
REFLECTOR BANDEDGE
AT 12.6μm WHERE T=10%
TOTAL ENERGY OUTPUT (mJ)
SPECTRAL PEAK-TO-REFLECTOR
BANDEDGE SEPARATION, Δλ (μm)
0
20
40
60
80
100
0
0.2
0.4
0.6
0.8
1.0

Figure 2

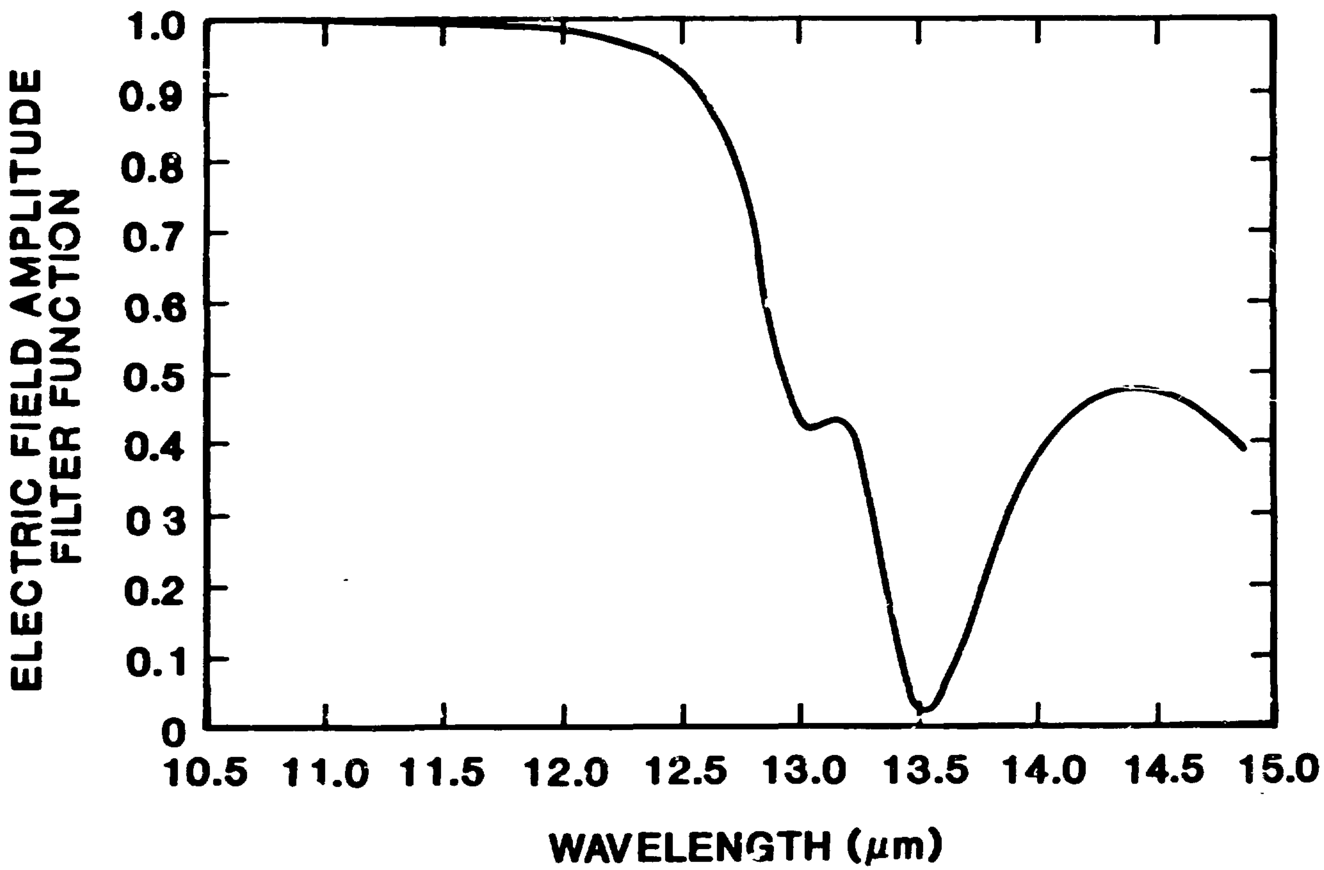

1.0
0.9
0.8
0.7
0.6
0.5
0.4
0 3
0.2
0.1
0
ELECTRIC FIELD AMPLITUDE FILTER FUNCTION
10.5 11.0 11.5 12.0 12.5 13.0 13.5 14.0 14.5 15.0
WAVELENGTH (μm)

Figure 3a

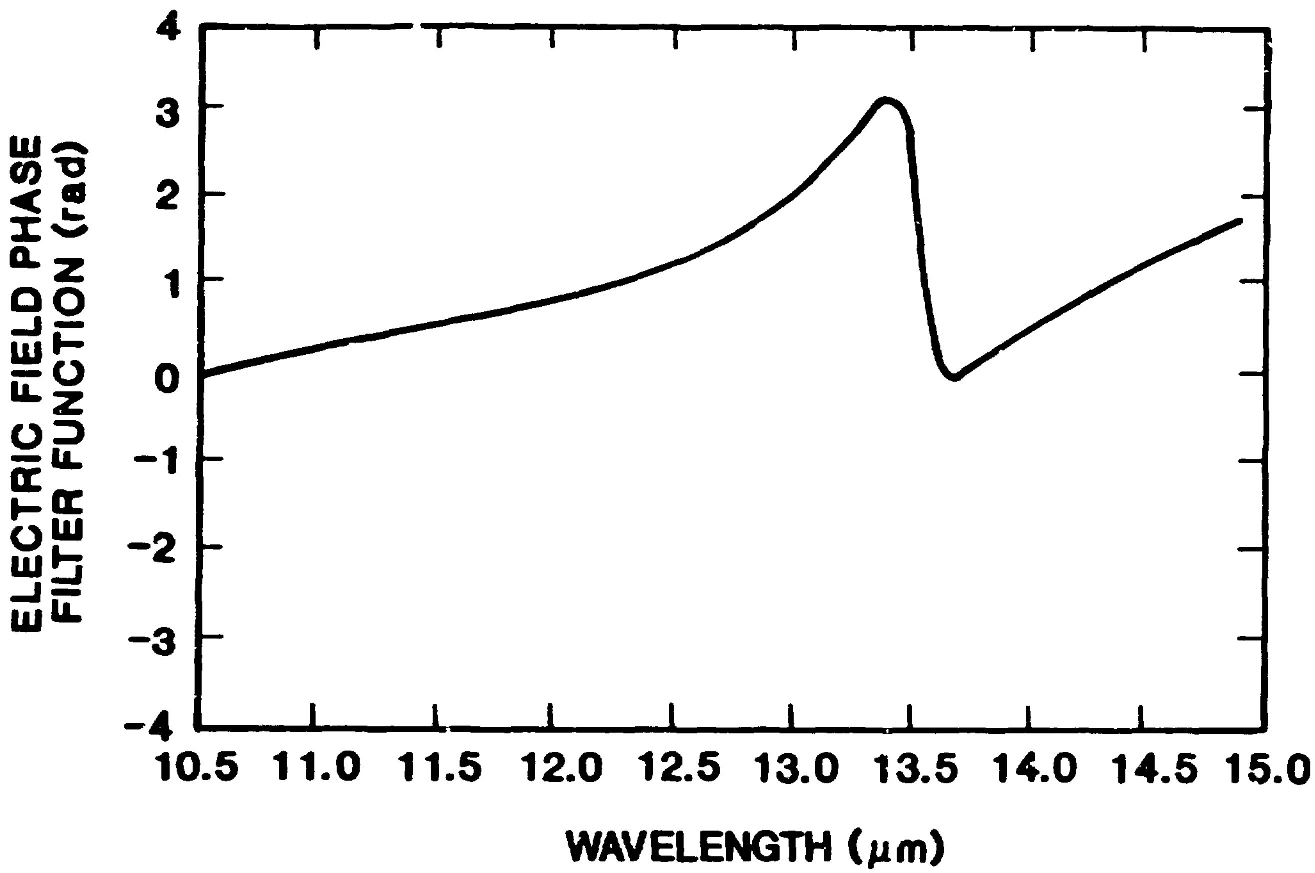

ELECTRIC FIELD PHASE
FILTER FUNCTION (rad)
4
3
2
1
0
−1
−2
−3
−4
10.5
11.0
11.5
12.0
12.5
13.0
13.5
14.0
14.5
15.0
WAVELENGTH (μm)

Figure 3b

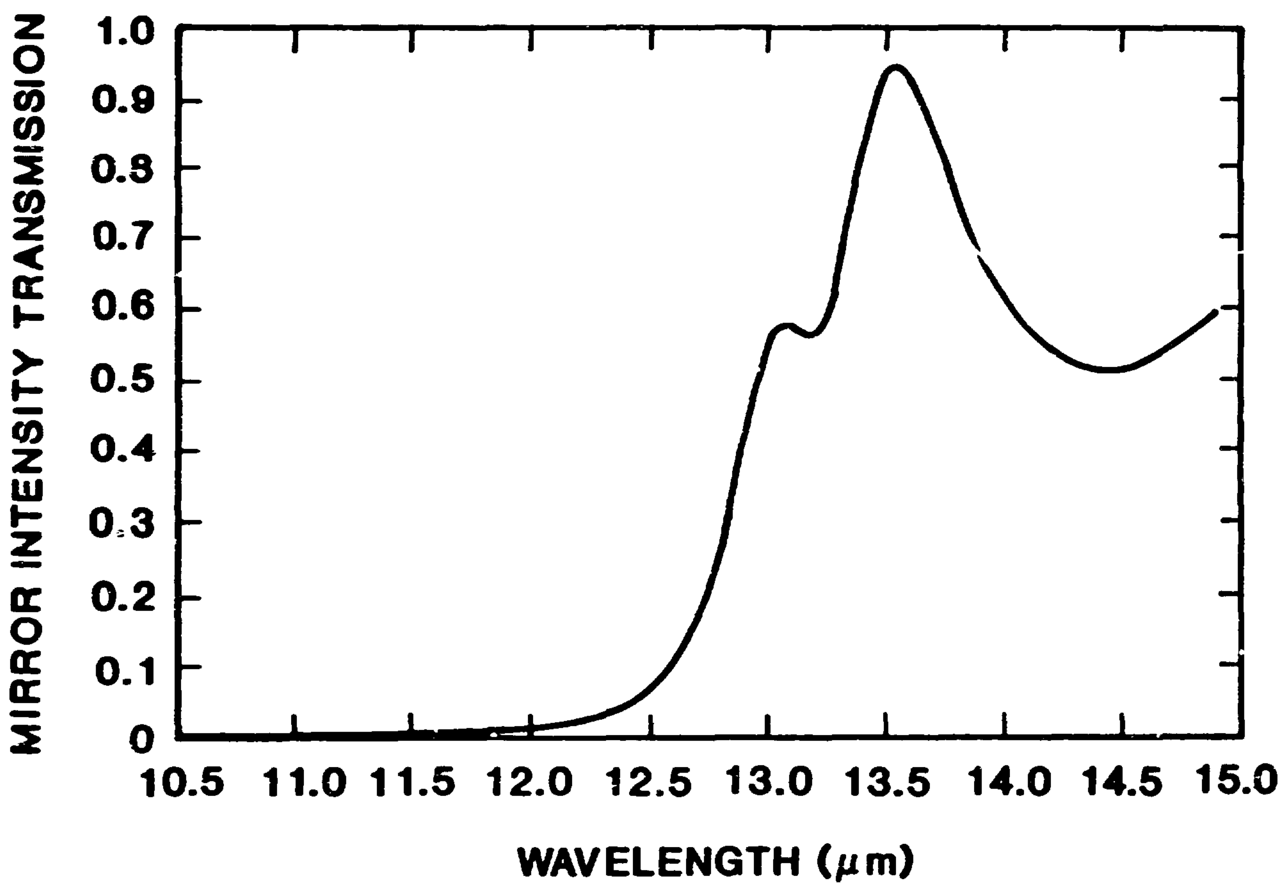
MIRROR INTENSITY TRANSMISSION
1.0
0.9
0.8
0.7
0.6
0.5
0.4
0.3
0.2
0.1
0
10.5
11.0
11.5
12.0
12.5
13.0
13.5
14.0
14.5
15.0
WAVELENGTH (μm)

Figure 3c

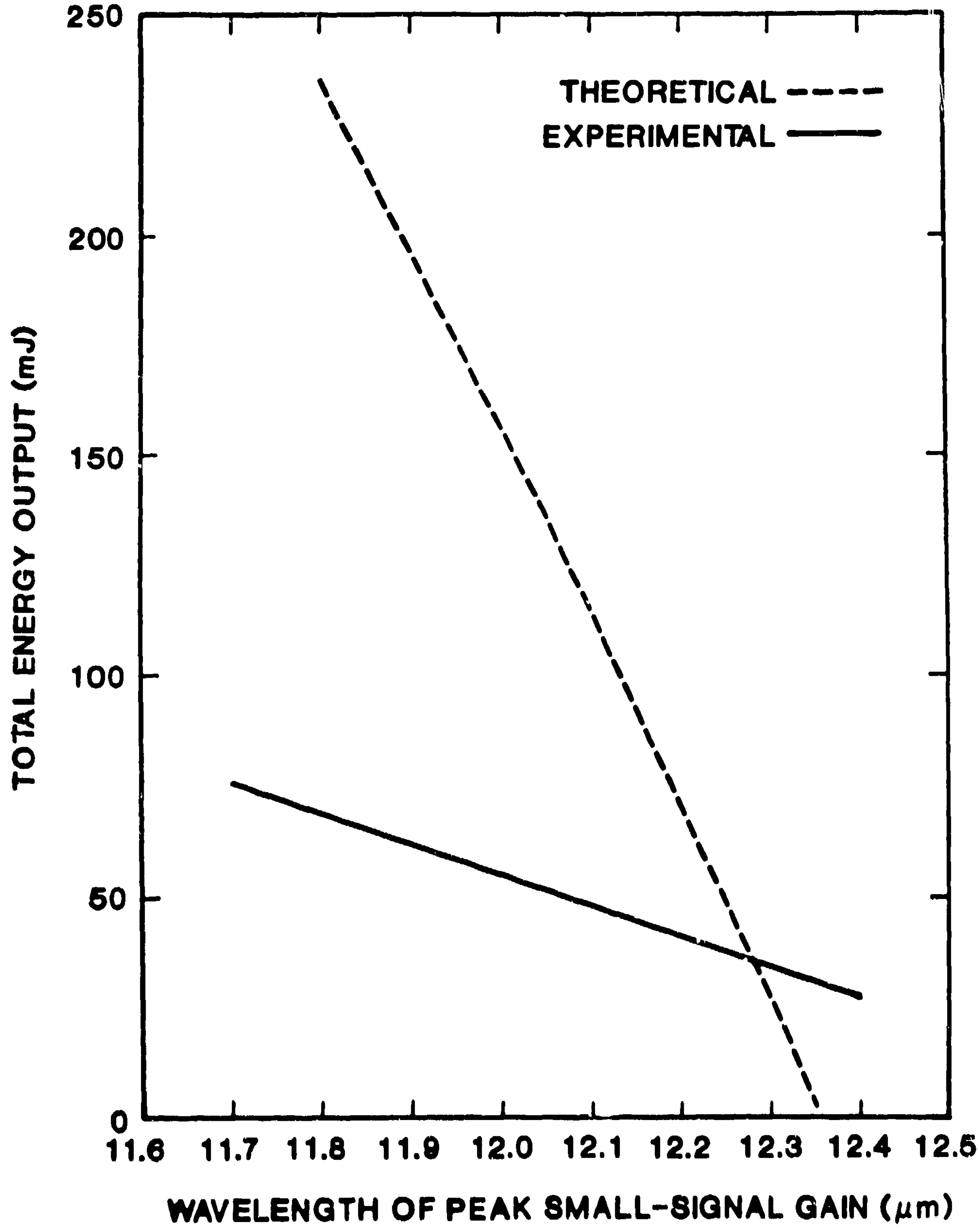
250
200
150
100
50
0
TOTAL ENERGY OUTPUT (mJ)
THEORETICAL
EXPERIMENTAL
11.6
11.7
11.8
11.9
12.0
12.1
12.2
12.3
12.4
12.5
WAVELENGTH OF PEAK SMALL-SIGNAL GAIN (μm)

Figure 4

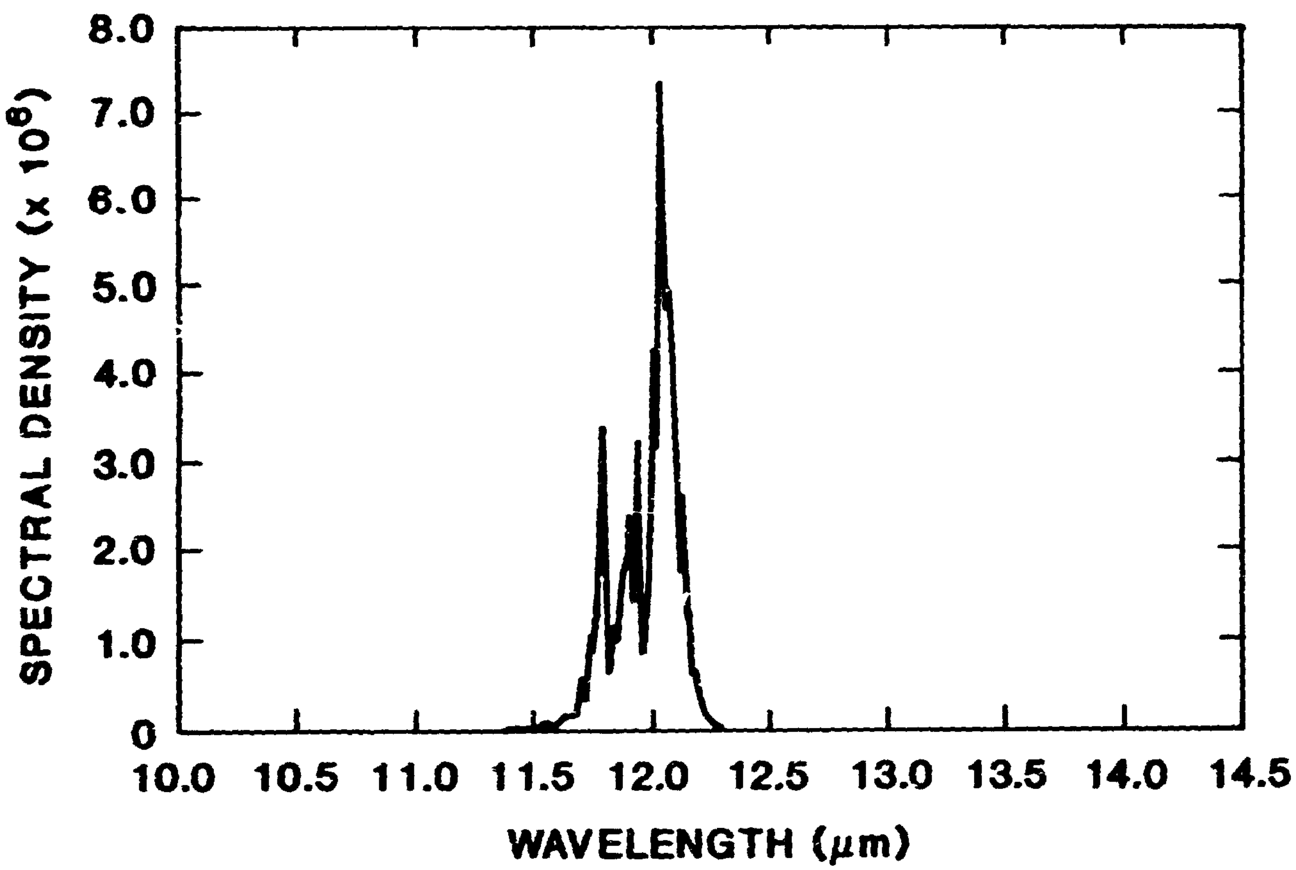
SPECTRAL DENSITY (x 10^6)
8.0
7.0
6.0
5.0
4.0
3.0
2.0
1.0
0
10.0
10.5
11.0
11.5
12.0
12.5
13.0
13.5
14.0
14.5
WAVELENGTH (μm)

Figure 5a

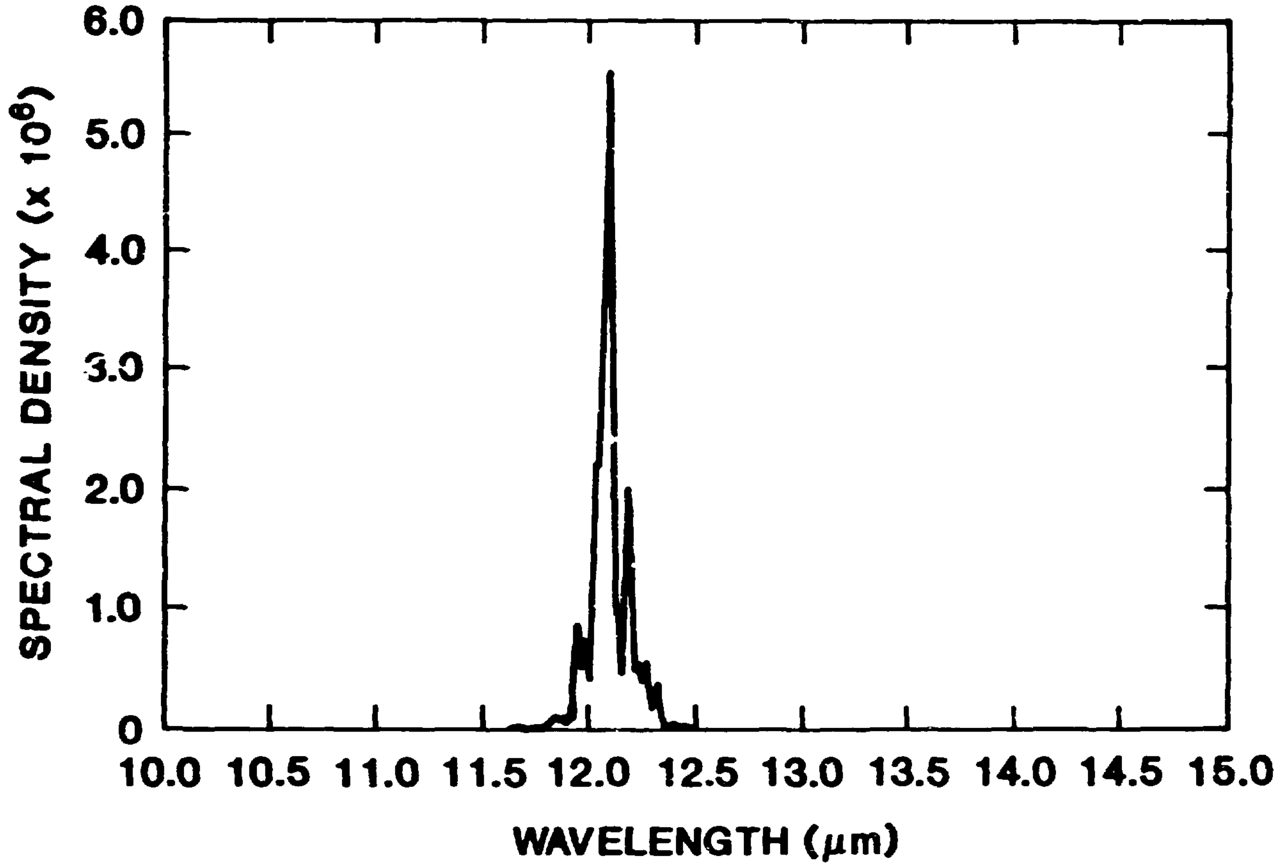
6.0
5.0
4.0
3.0
2.0
1.0
0
SPECTRAL DENSITY (x 10^6)
10.0
10.5
11.0
11.5
12.0
12.5
13.0
13.5
14.0
14.5
15.0
WAVELENGTH (μm)

Figure 5b

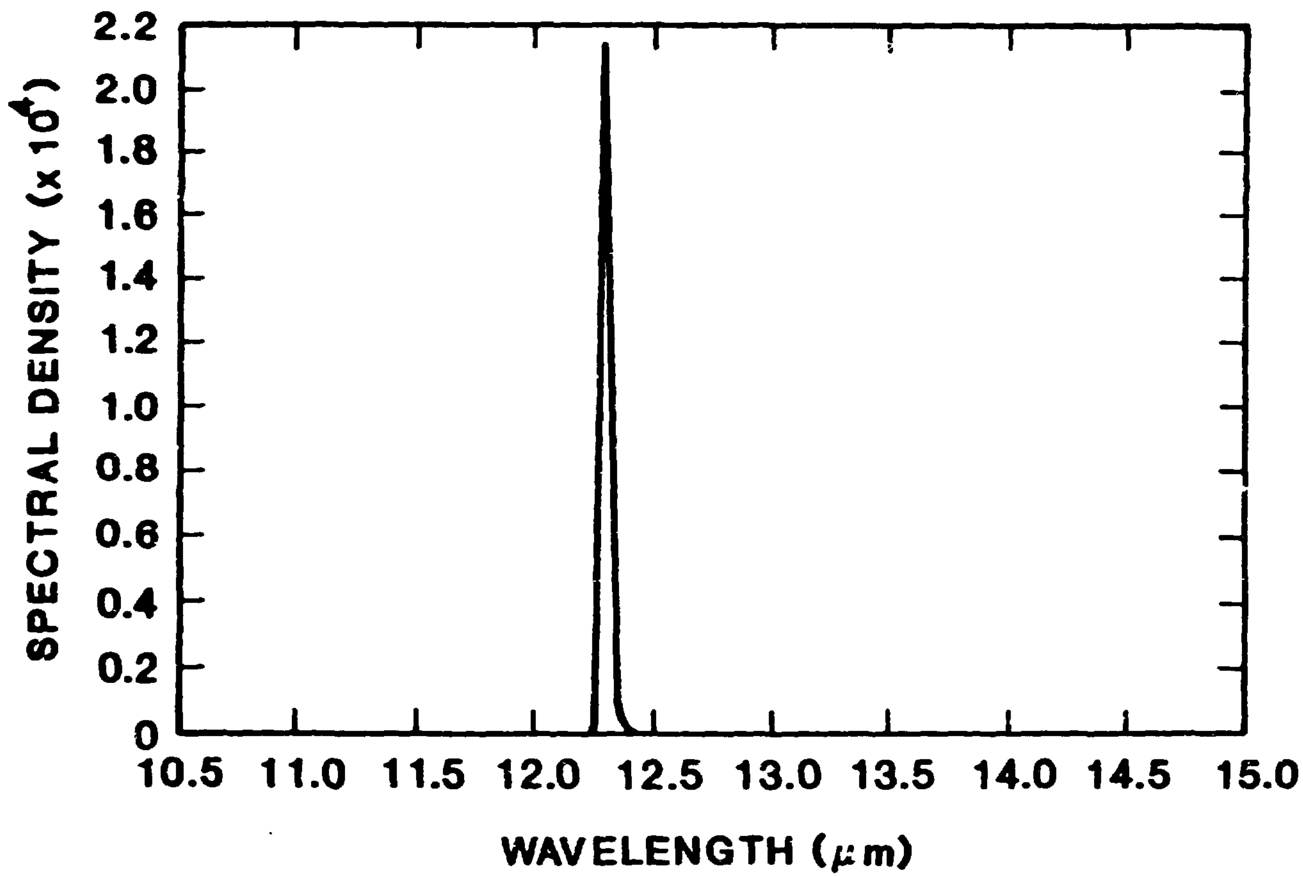
SPECTRAL DENSITY (x 10^4)
2.2
2.0
1.8
1.6
1.4
1.2
1.0
0.8
0.6
0.4
0.2
0
10.5
11.0
11.5
12.0
12.5
13.0
13.5
14.0
14.5
15.0
WAVELENGTH (μm)

Figure 5c

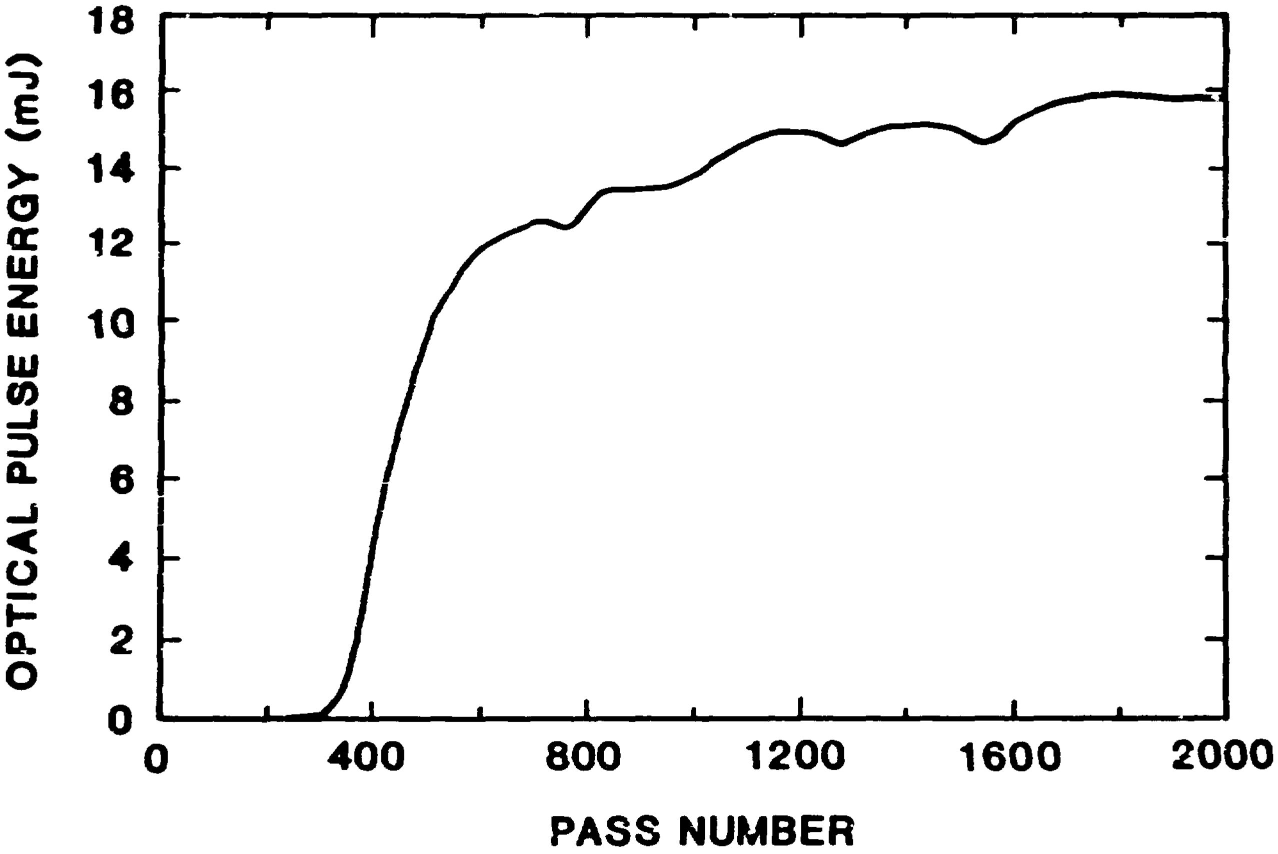
18
16
14
12
10
8
6
4
2
0
OPTICAL PULSE ENERGY (mJ)
0
400
800
1200
1600
2000
PASS NUMBER

Figure 6a

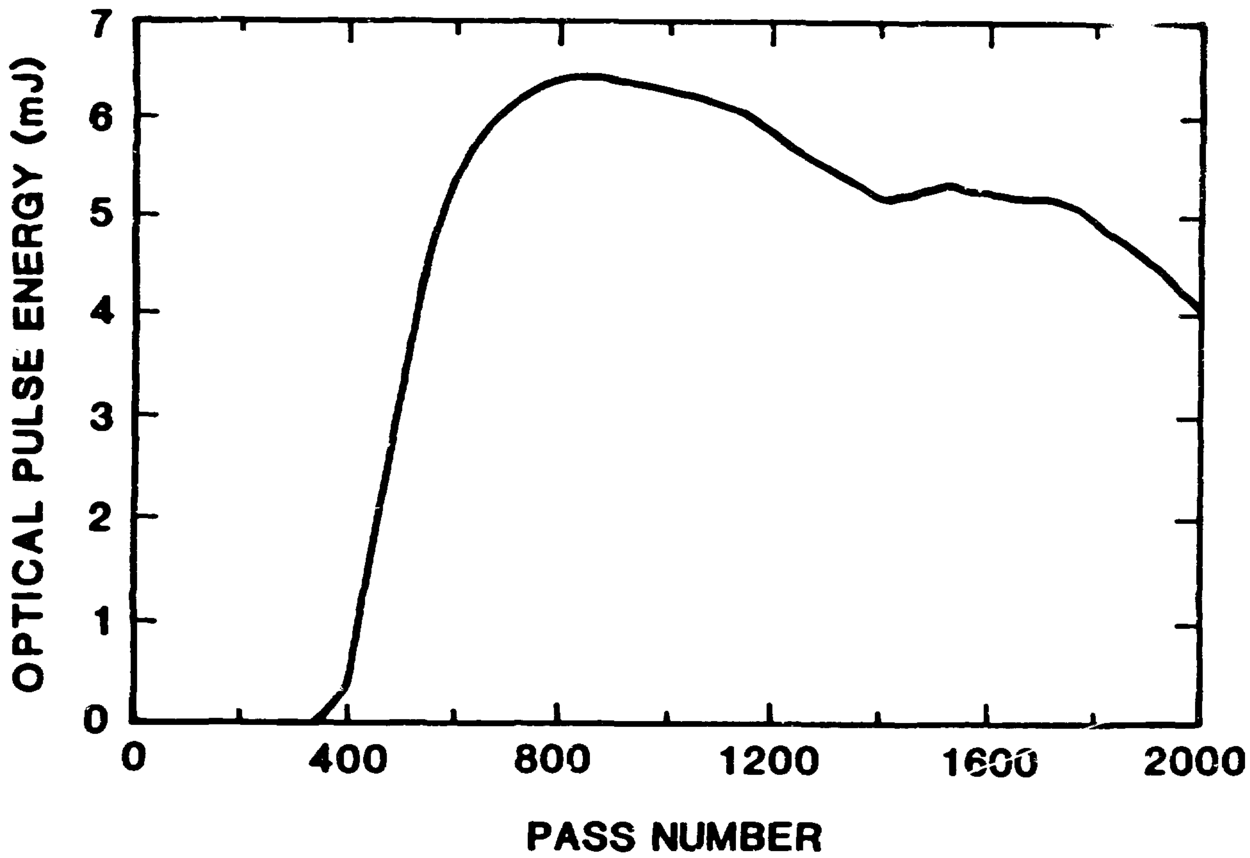
OPTICAL PULSE ENERGY (mJ)
7
6
5
4
3
2
1
0
0
400
800
1200
1600
2000
PASS NUMBER

Figure 6b

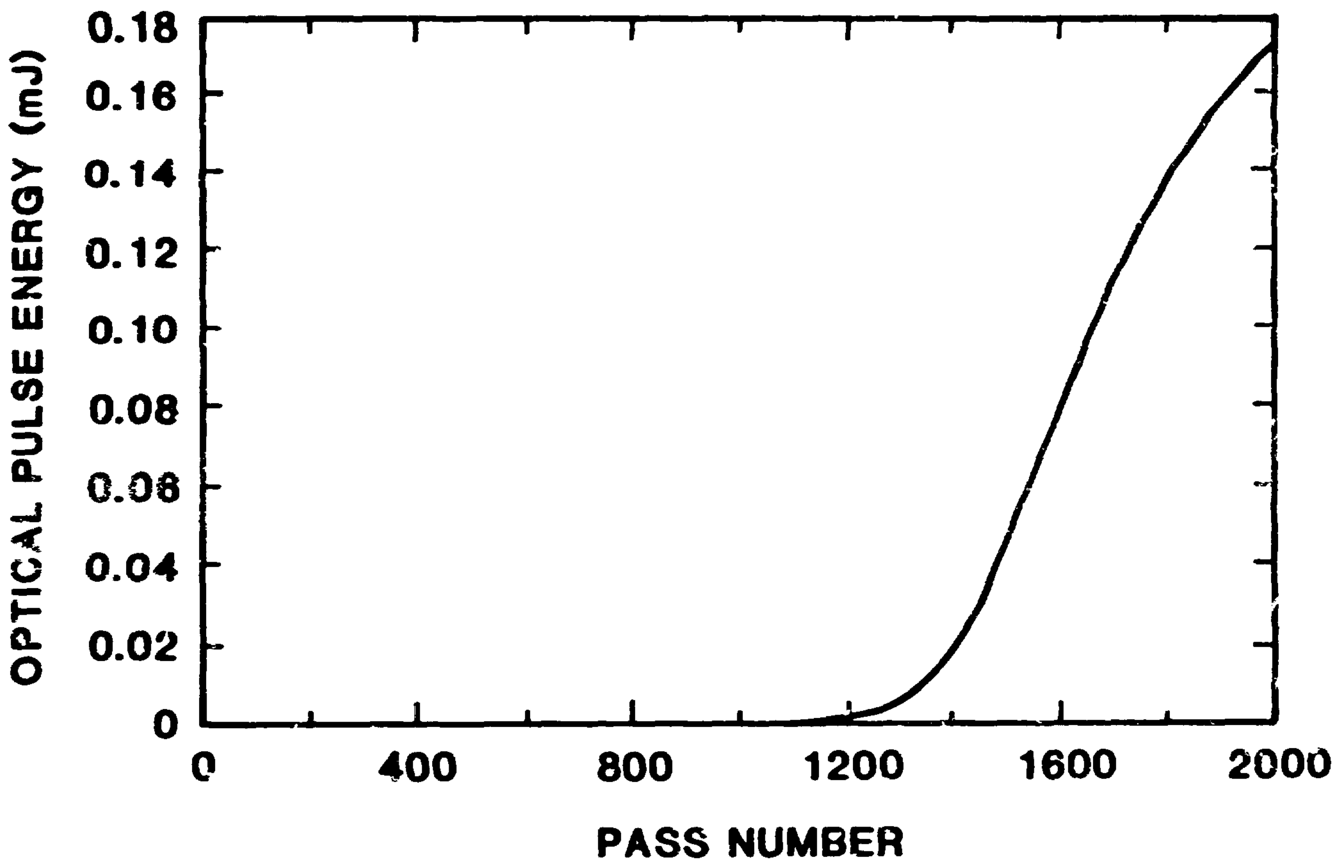

OPTICAL PULSE ENERGY (mJ)
0.18
0.16
0.14
0.12
0.10
0.08
0.06
0.04
0.02
0
0
400
800
1200
1600
2000
PASS NUMBER

Figure 6c